

ELECTRON COOLING IN THE RECYCLER COOLER

A. Shemyakin[#], L.R. Prost, FNAL*, Batavia, IL 60510, U.S.A.

A. Fedotov, BNL, Upton, NY 11973, USA

A. Sidorin, JINR, Dubna 141980, Russia

Abstract

A 0.1-0.5 A, 4.3 MeV DC electron beam provides cooling of 8 GeV antiprotons in Fermilab's Recycler storage ring. The most detailed information about the cooling properties of the electron beam comes from drag rate measurements. We find that the measured drag rate can significantly differ from the cooling force experienced by a single antiproton because the area of effective cooling is significantly smaller than the physical size of the electron beam and is comparable with the size of the antiproton beam used as a probe. Modeling by the BETACOOOL code supports the conclusion about a large radial gradient of transverse velocities in the presently used electron beam.

INTRODUCTION

Since the first demonstration of relativistic electron cooling in the Recycler Electron Cooler (REC) [1], cooling measurements of various types have been performed. In some, the cooling force was derived from the longitudinal distribution of the antiproton beam being in equilibrium with either IBS [1] or an external wide band noise source [2]. The most relevant figures of merit for operation, the cooling rates, were measured as changes of the time derivative of the longitudinal momentum spread and transverse emittances, when the electron beam is turned on [3]. In this paper, we concentrate primarily on drag rate measurements. First, we analyze the conditions, for which the measured drag rate correctly represents the cooling force experienced by a single antiproton, then present the results of the measurements, and compare them with simulations.

DRAG RATE AND COOLING FORCE

In a drag rate measurement, the electron energy is changed by a jump, and the time derivative of the average antiproton momentum, $\dot{\bar{p}}$, is recorded [4]. For a pencil-like antiproton beam with a small enough momentum spread, this derivative is equal to the cooling force applied to an antiproton with momentum offset $\delta p = \bar{p} - p_0$, where p_0 is the equilibrium momentum. Generally speaking, for the beam with finite emittances, the drag rate is given by integration over the 6D antiproton and electron distributions. For typical REC parameters, several simplified assumptions are valid:

- in the time of a drag rate measurement, the transverse antiproton distribution does not change, so

* FNAL is operated by Fermi Research Alliance, LLC under Contract No. DE-AC02-07CH11359 with the United States Department of Energy.

[#]shemyakin@fnal.gov

that transverse diffusion and cooling can be neglected for the longitudinal dynamics;

- the antiproton beam is axially symmetrical in the cooling section;
- direct effect of the transverse antiproton velocities is negligible, because the transverse electron velocities are much larger. Therefore, the cooling force depends on the radial position of an antiproton with respect to the electron beam center r but not on the antiproton transverse velocity.

In this case, the drag rate can be written as an integral of the non-magnetized cooling force over the radial and momentum antiproton distribution as follows:

$$\dot{\bar{p}} = \iint F(\delta W, \alpha_e, j_e, \Delta p) \cdot f(p, r) 2\pi \cdot r dr dp, \quad (1)$$

where the cooling force is shown dependent on the electron energy spread δW , angle α_e , and current density j_e averaged over the length of the cooling section, as well as on the antiproton momentum offset $\Delta p = p - p_0$.

Similarly, changes of the r.m.s. momentum spread

$$\sigma_p^2 = \iint (p - \bar{p})^2 \cdot f(p, r) 2\pi \cdot r dr dp$$

$$\frac{d}{dt} \sigma_p^2 =$$

$$D + 2 \iint F(\delta W, \alpha_e, j_e, \Delta p) \cdot f(p, r) \cdot 2\pi \cdot r dr dp, \quad (2)$$

where D is the longitudinal diffusion coefficient.

Dependence of the cooling force on the radius comes from the radial distributions of the current density and angles, while the electron energy spread is determined primarily by the terminal voltage fluctuations. If the electron beam is cold, its current density distribution in the cooling section follows the one on the cathode $j_{cath}(r_{cath})$:

$$j_e(r) = j_{cath} \left(r \cdot \sqrt{\frac{B_{cs}}{B_{cath}}} \right) \cdot \frac{B_{cs}}{B_{cath}}, \quad (3)$$

where B_{cs} and B_{cath} are the magnetic field magnitudes in the cooling section and at the cathode, respectively.

Gun simulations and Eq.(3) give for j_e a distribution close to parabolic in the main portion of the beam

$$j_e(r) \approx j_0 \cdot \left(1 - \frac{r^2}{a^2} \right), \quad (4)$$

with $j_0 = 0.96 \text{ A/cm}^2$ and $a = 2.9 \text{ mm}$.

Angles are composed of a component α_0 constant across the beam (associated with thermal velocities and dipole perturbations in the cooling section magnetic field) and a component linear with radius (caused by envelope scalloping), added in quadratures,

$$\alpha_e^2 = \alpha_0^2 \cdot \left[1 + \left(\frac{\alpha_b r}{\alpha_o r_b} \right)^2 \right] \equiv \alpha_0^2 \cdot \left[1 + \left(\frac{r}{b} \right)^2 \right]. \quad (5)$$

Taking into account that the first derivative of both above distributions is zero on axis, the first terms of the Taylor expansion of the cooling force over radius and momentum give

$$\dot{\vec{p}} \approx F(\delta p, 0) + \frac{\partial^2 F(\delta p, 0)}{\partial p^2} \cdot \frac{\sigma_p^2}{2} + \frac{\partial^2 F(\delta p, 0)}{\partial r^2} \cdot \frac{\sigma_r^2}{2}. \quad (6)$$

$$\sigma_r^2 = \iint r^2 \cdot f(p, r) 2\pi \cdot r \, dr \, dp$$

The drag rate is close to the cooling force experienced by an on-axis antiproton,

$$\dot{\vec{p}} \approx F(\delta p, 0), \quad (7)$$

when the terms with second derivatives are small. With the assumption that Eq.(7) was valid, the drag rate data $\dot{\vec{p}}(\delta p)$ presented in Ref.[4] (reproduced as data Set 1 in Fig.2 below) were fitted to the non-magnetized formula with a constant Coulomb logarithm L_c outside of the integral [5], and the second derivatives were calculated. For typical parameters ($\delta p = 1-20$ MeV/c, $\sigma_r \sim 0.5$ mm), the contribution of the second derivative terms in Eq.(6) is below 10% if $\sigma_p < 0.4$ MeV/c and the coefficient b from Eq.(5) is >2 mm. While the first restriction is comparatively easy to fulfill for the typical number of antiprotons in these measurements ($N_p \sim 4 \cdot 10^{10}$), we were not able to extract the correct value of b from direct measurements of the electron beam properties. However, this value can be roughly estimated from the radial dependence of the drag rate.

DRAG RATE MEASUREMENTS

The drag rates measured as a function of the parallel offset between the electron and antiproton beams are shown in Fig.1. ε_{Sch} and ε_{FW} indicate emittances measured with Schottky detectors and flying wires, correspondingly, in π mm-mrad, normalized, 95%, averaged for vertical and horizontal. The beta-function in the cooling section is 30 m. The solid curve in Fig.1 is $\sqrt{1 - (r/a)^2} / \sqrt{1 + (r/c)^2}$ with $a = 2.9$ mm, $c = 1.15$ mm and is shown for visual representation. The values of σ_r are estimated from ε_{FW} assuming a Gaussian distribution (unless noted otherwise).

The width of the measured distributions is significantly lower than 2 mm required for Eq. (7) to be valid. Indeed, for nearly identical electron beam parameters and, therefore, the same cooling force, the drag rate changes significantly with a decrease of the antiproton beam size. Most likely, the frequently observed effect of a decrease of the drag rate within a set of measurements (see sets 1 and 2 in Fig.1) is related to the creation of long low-intensity transverse tails that affect the drag rates, and which are measured with the Schottky detectors but not in ε_{FW} , which is extracted from the high-

background flying wire signals. Because the width of the curves of Fig.1 is comparable with the antiproton beam size, the radial dependence of the cooling force should be even sharper, so that at least $b \leq 1$ mm.

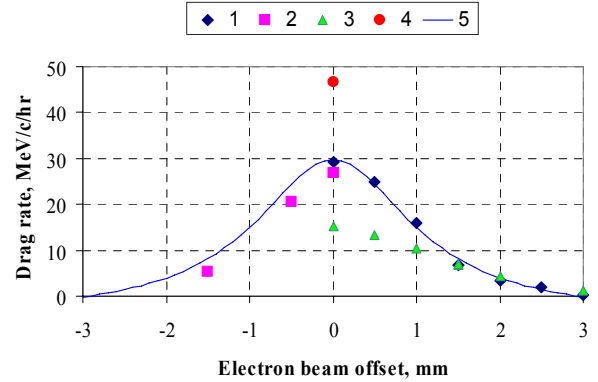


Figure 1: Drag rate as a function of the electron beam offset. Voltage jump was 2 kV, $I_e = 0.1$ A, $N_p = 4 \cdot 10^{10}$. Set 1: the antiproton beam was scraped to the radius in the cooling section of 1.1 mm, 25 min prior to the measurement. Set 2: negative offsets measured the same day 2 hours after the scrape. During both measurements, $\varepsilon_{FW} = 0.3-0.7$ ($\sigma_r \sim 0.5$ mm). Set 3: data of Feb. 2006, taken several hours after scraping. $\varepsilon_{Sch} = 1.5-3$. Point 4: drag measurement immediately after scraping to 1.1 mm. $\varepsilon_{FW} \sim 0.1-0.2$ ($\sigma_r \sim 0.3$ mm).

Data showing the dependence of the drag rate on the value of the voltage jump (re-calculated to δp in Fig.2) exhibit the same trend of an increasing drag rate for lower antiproton emittances. The data can still be fitted to the simple non-magnetized model (Table 1).

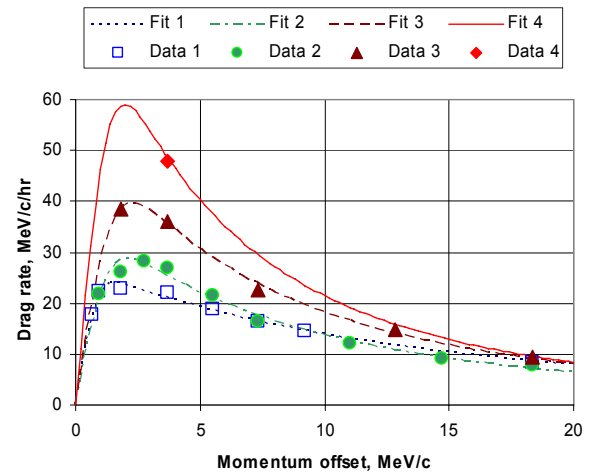


Figure 2: Longitudinal cooling force (negated) as a function of the antiproton momentum deviation. In all measurements, $I_e = 100$ mA, on-axis. In sets 2-4, transverse stochastic cooling was applied all time.

Table 1: Fitting parameters for the data shown in Fig.2 using the non-magnetized formula with a constant $L_c = 12$ outside of the integral.

Set	Date	Fitting parameters			Comments
		δW , eV	j_e , A/cm ²	α_e , mrad	
1	6-Feb-2006	370	1.1	0.20	No scraping. $\varepsilon_{Sch} = 1-2$
2	3-Jul-2007	550	0.60	0.12	4 hrs after scraping. $\varepsilon_{FW} = 0.3-0.7$
3	24-Jul-2007	620	0.71	0.11	Scraping for each point. $\varepsilon_{FW} < 0.5$
4	3-Jul-2007	550	0.64	0.09	After scraping to 1.1 mm

One of the consequences of the unevenness of the electron beam properties is an ineffective cooling of antiprotons with large transverse actions. Over time, this effect creates a strong correlation between the longitudinal and transverse tails of the antiproton distribution. Direct evidence is presented in Figure 3, showing a significant decrease of the momentum distribution width in the time of vertical scraping. Note that dispersion in the location of the scraper is small (~ 10 cm), and this effect was not observed while scraping a stochastically-cooled beam. This fact has operational consequences for the Recycler (see Ref. [6] and [7]).

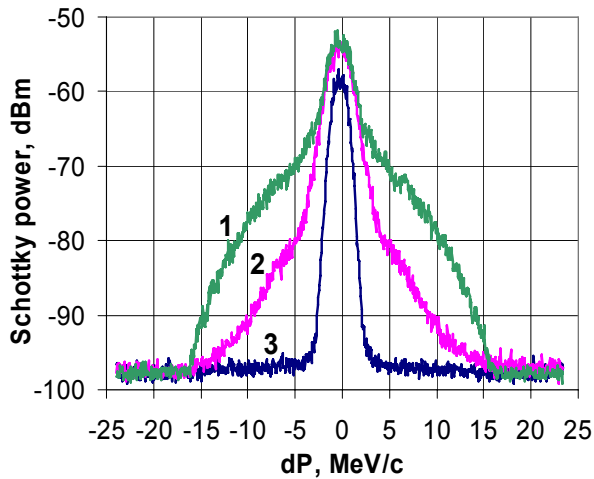


Figure 3: Evolution of the longitudinal 1.75 GHz Schottky profile of a deeply electron-cooled antiproton beam in the time of vertical scraping. For the curves 1, 2, and 3, the number of antiprotons, in units of 10^{10} , is 26, 20, and 4, and the offset of the vertical scraper re-calculated into a cooling section-equivalent position is 5.9, 2.1, and 1.7 mm, correspondingly. Before the scrape, antiprotons were cooled with a 0.1 A electron beam for ~ 40 min. $\varepsilon_{FW} = 0.7 \pi$ -mm-mrad (95%, n) at the start of the scrape.

COMPARISON WITH BETACOOOL

The measured cooling rates of an operational-intensity antiproton beam reported in Ref. [3] were compared with BETACOOOL [8] simulations (Figure 4). For these simulations, the measured drag rate (Set 1 in Fig.2) was interpreted as a cooling force and fitted to the non-magnetized formula with the Coulomb logarithm inside the integral. The fitted parameters were found to be $\delta W = 300$ eV, $\alpha_e = 0.11$ mrad, and the beam size a in Eq.(4), 3.5 mm for a 100 mA beam. These parameters were used to predict the cooling rates where the diffusion coefficients were adjusted to fit the slopes obtained before electron cooling was applied and the gradient of the angular spread was tuned to match the longitudinal rate (which gives $b = 2.1$ mm). The transverse cooling rate measured with flying wires was higher than the simulated one by a factor of two. The agreement was considered reasonably good because the transverse rate measured at the same time with Schottky monitors was almost 3 times lower than the FW's, and we do not have a complete explanation for this.

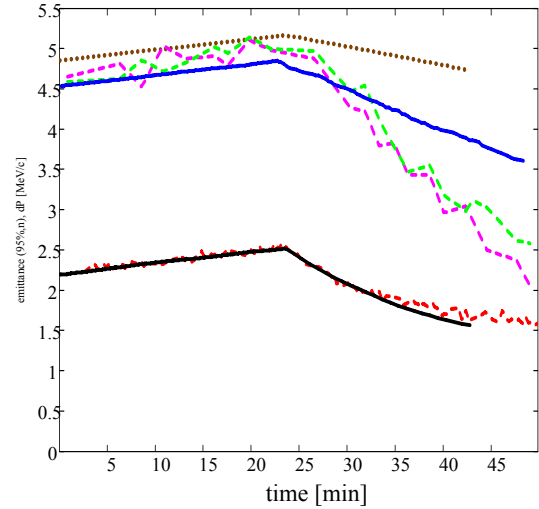


Figure 4: Comparison of measured cooling rates with simulation by the BETACOOOL code. Set 1 (lower curves): momentum spread - solid black line (simulations); dash red line (measurements). Set 2 (upper curves): emittance - dashed pink and green lines (FW horizontal and vertical measurements), solid blue line (simulations with Gaussian fit); dotted brown line (simulation with rms of full distribution with non-Gaussian tails). Electron beam was turned on at 23 min.

The evolution of the longitudinal profiles in a set of drag rate measurements at various electron beam currents was simulated as well. Fitting the data within measurement errors for both \ddot{p} and $\dot{\sigma}_p$ required $\alpha_0 = 0.09$ mrad and $b = 0.35$ mm. While these differ significantly from our previous estimations of the electron beam properties (for example, [4]), these numbers are in agreement with the data presented in the previous chapter and with recently found indications of large envelope

oscillations in the cooling section [7]. If correct, this interpretation means that the cooling force of an antiproton on axis can be noticeably higher than the measured drag rates and that a decrease of the angle gradient by careful adjustment of the envelope oscillations can increase the effective cooling rate in operation significantly.

CONCLUSION

1. The drag rate is equal to the cooling force experienced by a single antiproton when the electron beam properties are nearly constant across the antiproton beam. Analysis of the drag rate measurements show that this condition is not fulfilled in the Recycler cooler.
2. Most likely, the portion of the electron beam where electron cooling is effective is significantly decreased because of a large radial gradient of the electron transverse velocities.
3. Careful adjustment of envelope oscillations may eliminate that gradient and increase the cooling rates by several times.

ACKNOWLEDGMENTS

We are grateful to the entire Recycler department for the help with measurements and many discussions.

REFERENCES

- [1] S. Nagaitsev *et al.*, Phys. Rev. Lett. **96**, 044801 (2006)
- [2] D.R. Broemmelsiek and S. Nagaitsev, Proc. of EPAC'06, Edinburgh, UK, June 26-30, 2006, p.1241
- [3] L.R. Prost and A. Shemyakin, Proc. of PAC'07, Albuquerque, U.S.A., June 2007, p. 1715.
- [4] L. Prost *et al.*, in Proc. of HB2006, Tsukuba, Japan, May 29-June 2, 2006, WEAY02, p 182
- [5] Ya.S. Derbenev and A.N. Skrinsky, Particle Accelerators **8** (1977) 1
- [6] L.R. Prost *et al.*, this conference
- [7] A. Shemyakin *et al.*, this conference
- [8] I.N. Meshkov *et al.*, Physics guide of BETACOOL code, v.1.1, BNL note C-A/AP#262